Circulation Journal
Circ J 2022; 86: 966–974
doi:10.1253/circj.CJ-21-0649

ORIGINAL ARTICLE

Vascular Injury After Stenting
— Insights of Systemic Mechanisms of Vascular Repair —

Pilar Jimenez-Quevedo, MD, PhD; Esther Bernardo, BSc; Maria del Trigo, MD, PhD; Shuji Otsuki, MD; Luis Nombela-Franco, MD, PhD; Salvatore Brugaletta, MD, PhD; Arancha Ortega-Pozi, BSc; Raul Herrera, MD; Pablo Salinas, MD, PhD; Ivan Nuñez-Gil, MD, PhD; Hernan Mejía-Rentería, MD, PhD; Fernando Alfonso, MD, PhD; Cristina Fernandez-Perez, MD, PhD; Antonio Fernandez-Ortiz, MD, PhD; Carlos Macaya, MD, PhD; Javier Escaned, MD, PhD; Manel Sabate, MD, PhD; Nieves Gonzalo, MD, PhD

Background: The role of circulating progenitor cells (CPC) in vascular repair following everolimus-eluting stent (EES) implantation is largely unknown. The aim of the study was to investigate the relationship between temporal variation in CPC levels following EES implantation and the degree of peri-procedural vascular damage, and stent healing, as measured by optical coherence tomography (OCT).

Methods and Results: CPC populations (CD133+/KDR+/CD45low) included patients with stable coronary artery disease undergoing stent implantation, and were evaluated using a flow cytometry technique both at baseline and at 1 week. OCT evaluation was performed immediately post-implantation to quantify the stent-related injury and at a 9-month follow up to assess the mid-term vascular response. Twenty patients (mean age 66±9 years; 80% male) with EES-treated stenoses (n=24) were included in this study. Vascular injury score was associated with the 1-week increase of CD133+/KDR+/CD45low (β 0.28 [95% CI 0.15; 0.41]; P<0.001) and with maximum neointimal thickness at a 9-month follow up (β 0.008 [95% CI 0.0004; 0.002]; P=0.04). Inverse relationships between numbers of uncoated and apposed struts for the 9-month and the 1-week delta values of CD133+/KDR+/CD45low (β –12.53 [95% CI –22.17; –2.90]; P=0.011), were also found.

Conclusions: The extent of vessel wall injury influences early changes in the levels of CPC and had an effect on mid-term vascular healing after EES implantation. Early CPC mobilisation was associated with mid-term strut coverage.

Key Words: Circulating progenitor cells; Drug-eluting stent; Optical coherence tomography; Restenosis; Stent thrombosis

The incidence of in-stent restenosis and stent thrombosis – the main causes of stent failure following percutaneous coronary intervention (PCI) – has been reduced with the development of and treatment with second-generation drug-eluting stents (DES).[1] Nevertheless, a percentage of patients still experience these complications, which may have clinically relevant consequences.

In the DES era, the biochemical and cellular mechanisms involved in ISR are largely unknown. Previous pathology reports have demonstrated a direct correlation between vascular damage during stent implantation and the reparative response of the vascular wall;[2] an inadequate response may lead to significant luminal obstruction. Vascular healing after stenting results from the combined effect of local and systemic responses to vessel damage. The latter includes the mobilisation of cellular precursors such as bone marrow-derived progenitor cells (BM-PC),[3] whose presence in the neointimal tissue generated after vascular damage has been documented.[4] Several clinical studies have shown a relationship between levels of circulating progenitor cells (CPC) and ISR occurrence following the implantation of bare metal stents (BMS),[5–8] an effect that might be explained by the ability of CPC to differentiate not only as endothelial cells, but also as smooth muscle cells (SMC) with synthetic phenotype.[9] From the perspective of these findings, CPC levels can be considered risk biomarkers for ISR development following BMS implantation. In addition,

Editorial p 975

Received July 26, 2021; revised manuscript received October 6, 2021; accepted October 20, 2021; J-STAGE Advance Publication released online December 2, 2021 Time for primary review: 30 days

Clinico San Carlos University Hospital, IdISSC, Madrid (P.J.-Q., E.B., M.d.T., L.N.-F., A.O.-P., R.H., P.S., I.N.-G., H.M.-R., F.A., C.F.-P., A.F.-O., C.M., J.E., N.G.); University Hospital Clínic, Institut d'Investigacions Biomèdiques August Pi i Sunyer (IDIBAPS), Barcelona (S.O., S.B., M.S.), Spain

Mailing address: Pilar Jimenez-Quevedo, MD, PhD, Interventional Cardiology Department, Hospital Clinico San Carlos, IdISSC, c/Martín Lagos s/n, 28040 Madrid, Spain. E-mail: patropjq@gmail.com

ISSN-1346-9843

the percentage of BM-PC in histological sections of neointima varies according to the type of vascular damage, leading to a hypothesis that the magnitude of the systemic response and the recruitment of BM-PC in the stented coronary segment might be modulated by the extent of vascular injury.[10]

The aim of our study was to investigate the association between the systemic response measured by temporal variation in CPC levels to the degree of acute vessel wall injury caused by everolimus-eluting stent (EES) implantation, as measured by optical coherence tomography (OCT). In addition, we also studied the relationship between CPC levels and mid-term vascular repair mechanisms: strut coverage and neointimal hyperplasia.

Methods

Study Population and Endpoints

This prospective, single-centre, observational, longitudinal study collected individual data from an opportunistic sample of patients with coronary artery disease treated by EES implantation and fulfilled the following inclusion criteria: clinical presentation with stable angina, silent ischemia or unstable angina (with no elevation of markers of myocardial damage); presence of at least 1 severe coronary stenosis (>70% diameter stenosis by visual analysis) amenable to percutaneous treatment with DES implantation and OCT interrogation; and chronic treatment with statins for at least 2 months prior to study inclusion. Exclusion criteria were: age <18 years; pregnant, or of childbearing potential; recent (<3-month) ST-segment or non ST-segment elevation myocardial infarction; additional DES or BMS implanted during the same procedure; percutaneous treatment of restenotic lesions or total chronic occlusions; use of ablation techniques (rotational atherectomy); chronic renal insufficiency with serum creatinine ≥2.5 mg/dL; coronary revascularisation in the previous 3 months; severe ventricular dysfunction (LVEF <25%); major trauma or surgery in the previous 3 months; organ transplant recipient; active neoplastic process or inflammatory disease; treatment with immunosuppressants; contraindication or allergy to thienopyridines; and <1-year life expectancy. All patients were treated with dual anti-platelet therapy up to 1 year.

The local ethics committee approved the study protocol, and all patients provided written informed consent to undergo the procedure and to be included in the study.

As we study different vascular healing processes both acute (vascular injury) and in the longer term (strut coverage and neointimal hyperplasia) following DES implantation, we studied CD133+/KDR/CD45low, which are immature cells (CD133+) and are committed to the endothelial lineage, as expressed by the KDR+ marker.[10]

The primary endpoint of the study was to identify any association between CPC mobilization after EES implantation and its relationship with the extent of vascular injury after stenting, as measured by OCT. Secondary endpoints aimed to assess the mobilization of progenitor cells and the degree of strut coverage at 9-month follow up; the association between the degree of vascular injury and neointimal hyperplasia at 9 months was also assessed.

Flow Cytometry Analysis and Colony-Forming Unit Assay

All flow cytometry analysis was performed, as previously described.[5] Briefly, peripheral blood samples were taken and placed into EDTA-anticoagulant tubes. Samples were obtained before stent implantation and at 7 days. A total of 100 μL whole blood was labelled with fluorescein isothiocyanate (FITC)-CD45 antibody (Miltenyi Biotec, Germany), Alexa Fluor 700 KDR (R&D Systems Minneapolis, MN, USA), Phycoerytrin-Cyanine-7 (PC7)–CD34 (Beckman Coulter, Miami, FL, USA), or phycoerythrin (PE)-CD133 antibody (Miltenyi Biotec) for 20 min on ice, then a lysis of erythrocytes was performed with VersaLyse (Beckman Coulter, CA, USA). Appropriate fluorescence isotype antibodies were used as controls. To determine absolute values, 100 μL of flow-count beads (Beckman Coulter) were added to each sample, and samples were immediately analysed using a Gallios flow cytometer (Beckman Coulter). At least 250,000 events were acquired in leukocyte gates. Cells were analysed using gating strategies according to the Modified ISHAGE Protocol.[11] Gate R1 corresponds to CD45+ events (including both CD45low and CD45bright events) and was displayed on CD45-FITC vs. a side scatter (SSC) dot plot. The events in gate R1 were displayed on CD133 vs. a SSC dot plot to identify CD133+ cells (R2 gate) according to labelling strategies. The third plot corresponds to cells with characteristic low CD45 fluorescence and a SSC dot plot (R3) that was plotted with R1 and R2 criteria. A forward scatter FSC and SSC dot plot was displayed to confirm that selected cells corresponded to the lymphocyte region (R4). Finally, the events fulfilling all criteria gates (R1, R2, R3 and R4) were displayed on a quadrant plot to define CD133+ and KDR+ cells. Data were analysed using Kaluza software (Beckman Coulter). The results were expressed as absolute numbers of cells per μL. Intraobserver variability was assessed by analysing in duplicate, and by using the same observer; the kappa-value obtained was 0.92.

A colony forming unit assay was performed to isolate mononuclear cells; 30 mL of EDTA-treated peripheral blood was diluted with the same volume of sterile saline solution. The diluted blood was centrifuged in Ficoll Density gradient (LSM 1077) at 1,200 rpm for 20 min at 20°C. Buffy coat (mononuclear fraction of cells) was collected and washed twice with physiological saline by centrifuging at 1,500 rpm for 15 min. The sediment was resuspended in MV2 endothelial cell culture (Promocell) with 50 μg/mL of gentamicin to obtain isolated mononuclear cell cultures, which were then seeded in plates coated with 10 μg/mL of human fibronectin. The plates were incubated at 37°C and 5% de CO_2 for the analysis of colony-forming units (CFU), a clustering of spindle cells distributed around a nucleus of rounded cells. On the following day, the supernatant of the culture plates with non-adherent cells was carefully collected and passed to new plates coated with fibronectin; these were kept under the same culture conditions for 1 week. At 7 days, the CFU were counted with an inverted optical microscope. The analysis of CFU was performed at baseline.

Quantitative Angiographic Analysis (QCA)

QCA analyses were performed to calculate the stent/artery ratio. The analysis was undertaken following a previously described methodology[12] using an automatic edge detection system (Medis Medical Imaging Systems BV Leiden, The Netherlands), by an investigator blinded to the clinical and laboratory data.

OCT Assessment

During PCI, OCT imaging was performed only after stent implantation and was used to guide stenting and to ensure

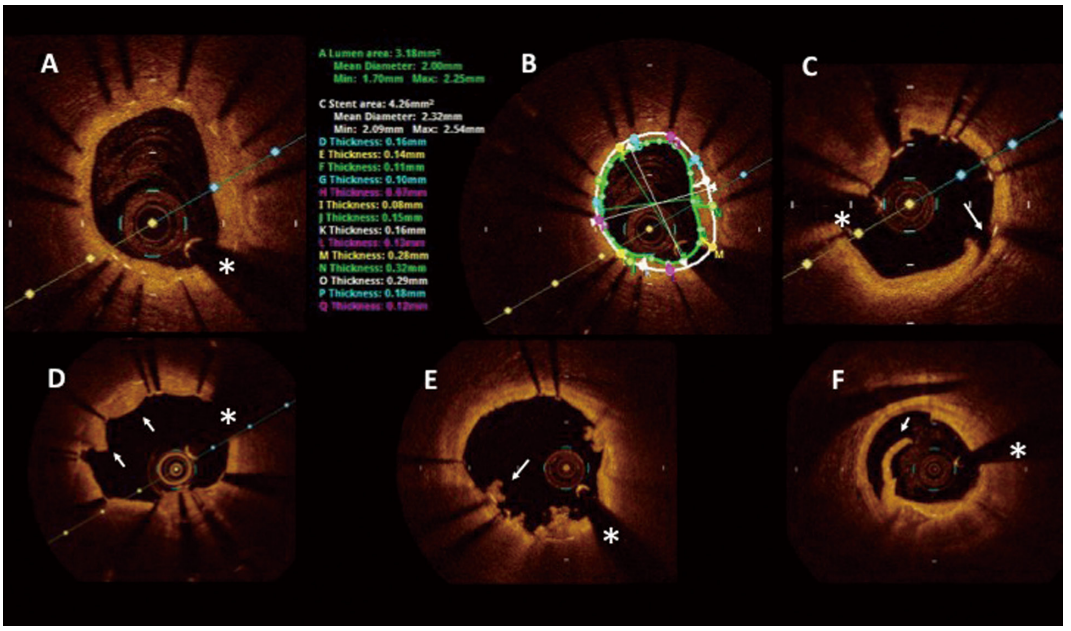

Figure 1. An example of optical coherence tomography (OCT) analyses of neointimal hyperplasia (**A**,**B**) and vascular damage (**C**–**F**). (**A**) OCT findings with mild neointimal hyperplasia at 9 months. (**B**) Computerized off-line analysis of the amount of neointimal hyperplasia. OCT analysis of the vascular damage after stent implantation: (**C**) intrastent dissections (arrow). (**D**) Plaque prolapse (arrow). (**E**) Thrombus (arrow). (**F**) Edge dissection (arrow). *Wire artifact.

adequate expansion and apposition of the implanted EES. Once PCI was completed, a set of OCT images was obtained for the purpose of the study. At 9 months follow up, the same coronary segment was again interrogated with OCT. The images were analysed offline at an independent core-lab (Barcicore Lab, Barcelona, Spain) by 2 independent observers blinded to blood analysis results using a workstation with dedicated OCT analysis software (LightLab Imaging Inc). The inter- and intra-observer variability of the data was excellent, with a k-value of 0.956 and 0.986, respectively. The region of interest comprised both the stented region and the stent margins (vessel segment 5 mm proximal and distal to the newly implanted stent after final post-dilatation). The procedural strategy adopted by operators to treat incomplete stent apposition (ISA) immediately after implantation was used to post-dilate in cases of large ISA distance (>350–400 μm).[13]

Assessment of Strut Coverage and Apposition

The OCT images obtained at follow up were analysed to determine whether stent struts were covered and apposed to the vessel wall. Struts were classified as uncovered and malapposed, as previously described.[14] In every 5th frame (1 mm), we evaluated each stent strut condition for classification into 1 of 6 categories: (1) well-apposed to the vessel wall with tissue coverage overlaying the strut; (2) well-apposed to the vessel wall without tissue coverage; (3) malapposed to the vessel wall with tissue coverage; (4) malapposed to the vessel wall without tissue coverage; (5) orifice branch site with tissue; and (6) orifice branch site without tissue. To normalize by stent length, we calculated the percentage of uncovered struts per mm of stent. Quantitative measurements included the neointimal area and the percentage area of neointimal tissue.[14] Neointimal volume was calculated as: neointimal area×stent length.

Assessment of Vessel Injury

In the post-implantation OCT images, acute vessel injury was evaluated, as previously described.[15] Tissue prolapse was defined as a convex-shaped protrusion of tissue between adjacent stent struts towards the lumen, without disruption of the continuity of the luminal vessel surface (**Figure 1D**). Protrusion of tissue between struts was considered as tissue prolapse only if the distance from the arc connecting adjacent stent struts to the greatest extent of protrusion was ≥50μm. The inter- and intra-observer variability of the data had a k-value of 0.965 and 0.983, respectively. Intra-stent dissection was defined as a disruption of the luminal vessel surface in the stent segment. It can appear in 2 forms: (1) dissection: the vessel surface is disrupted, and a dissection flap is visible; and (2) cavity: the vessel surface is disrupted, and an empty cavity can be seen (**Figure 1C**). The inter- and intra-observer variability of the data had a k-value of 0.943 and 0.981, respectively. Edge dissection was defined as a disruption of the luminal vessel surface in the edge segments (within 5 mm proximal and distal to the stent, no struts are visible; **Figure 1F**). The inter- and intra-observer variability of the data had a k-value of 0.9572 and 0.989, respectively. Thrombus was defined as an irregular mass with dorsal shadowing protruding in the lumen (mural thrombus) or a luminal mass with dorsal shadowing (**Figure 1E**). The inter and intra-observer variability of the data had a k-value of 0.965 and 0.987, respectively. In order to categorise the degree of vascular injury, we have used 2 definitions: (1) Injury score: this was calculated as previously described[16,17] for each

quadrant of each image (total injury score by frame from 0 to 8: 0=absence of dissection, 1=minor dissection [<300 μm in depth] and 2=major dissection [≥300 μm in depth]). Subsequently, stent-level injury score was calculated as a mean of the injury score of individual frames (also from 0 to 8), and vascular damage score was defined as the sum (1–4) of the presence of 4 individual variables: tissue prolapse, intra-stent dissections, dissection at the edges of the stent, and thrombi. Both scores were calculated at 1-mm intervals along the total stent length, and vascular damage also included both edges (5 mm).

Statistical Analysis

Continuous variables were presented as mean and standard deviation, or median and interquartile range in case of asymmetry, and categorical variables as percentages. After checking for normal distribution (Kolmogorov-Smirnov normality test), continuous variables were compared using a paired Student's t-test (comparison between baseline and follow up). To take into account intraindividual variability (repeated assessments), all comparisons were adjusted in a generalised estimating equations (GEE) model, stratifying per patient and per lesion. The slope of relationship β between the studied variables was calculated.

Statistical analysis was performed using STATA software (version 12.0) and reported P values were 2-sided. We assumed significance at the 5% level (P<0.05). An intermediate analysis of available data from the first 9 patients was used to calculate the final sample size; the correlation between the degree of neointimal hyperplasia measured by OCT and the change in CPC levels at 1 week was 0.548. With an alpha error of 0.05 and a beta error of 0.20, the calculated sample size was 19 patients treated with EES.

Results

Baseline and Procedural Characteristics

From 2012 to 2014, the study enrolled an opportunistic sample of 20 patients (24 lesions). Baseline characteristics are shown in **Table 1**. Mean age was 66±9 years and 80% were male. Seventy-six percent of the lesions were predilated and 60% were post-dilated. With the exception of 5 patients, the post-dilatation was performed prior to OCT evaluation, based on the angiographic and the Stent Boost imaging; therefore, these patients had 1 OCT run performed. In the remaining 5 lesions, post-dilatation was performed due to significant stent malapposition and a second OCT run was performed following this.

Table 1. Baseline Patient, Angiographic and Procedural Characteristics

Clinical characteristics (n=20)	
Age (years)	66±9
Female sex – No (%)	4 (20)
Risk Factors – No (%)	
Diabetes mellitus	6 (30)
Insulin-dependent diabetes	3 (15)
Hyperlipidemia	15 (75)
Hypertension	15 (75)
Ever smoked	11 (55)
Clinical status – No (%)	
Stable angina	12 (60)
Silent ischemia	8 (40)
Previous myocardial infarction	4 (20)
Previous CABG	0 (0)
Previous revascularization	4 (20)
Previous stroke, n (%)	4 (20)
Peripheral vasculopathy, n (%)	3 (15)
Renal insufficiency, n (%)	3 (15)
Ejection fraction (%)	57±9
Number of diseased vessels, mean ± SD	1.9±0.8
Multivessel PCI, n (%)	4 (20)
Treatment	
Statins, n (%)	20 (100)
ACEi/ARBs	20 (100)
Lesion characteristics (No. lesions=24)	
Treated artery, n (%)	
Left anterior descending	11 (44)
Left circumflex	4 (16)
Right coronary	10 (40)
Lesion length, mm	17.6±7
Moderate-severe calcification, n (%)	9 (36)
B2/ C class lesion, n (%)	11 (44)
Procedural characteristics	
Predilatation, n (%)	19 (76)
Postdilatation, n (%)	15 (60)
Stent length (mm)	21±8
Stent diameter (mm)	3.0±0.5
Maximal pressure (atm)	18±3
Inflation time (s) (+)	37±25
Maximal balloon diameter (mm)	3.33±0.6
Angiographic success, n (%)	25 (100)

Data are presented as n (%) or mean ± SD unless otherwise stated. ACEi/ARBs, angiotensin-converting enzyme inhibitors/ angiotensin II receptor blockers; CABG, coronary artery bypass graft; PCI, percutaneous coronary intervention.

OCT Analysis

All 24 lesions underwent a vascular damage analysis, and paired analysis was possible for 21 lesions; follow-up OCT images were unavailable for 3 lesions. At 9 months follow up, significant reductions were observed in mean luminal area, due to a significant increase in neointimal hyperplasia (**Table 2**). A total of 5,511 struts were evaluated by OCT (**Table 3**). At 9 months, only 0.30% showed malapposition without neointimal coverage.

Vascular Damage and CPC Levels

At 1 week, vascular damage and injury score were associated with the increase in the number of CD133+/KDR+/CD45low and also with the absolute number (**Table 4**, **Figure 2A**,**C**). Analysis of the different vascular damage components showed several significant associations: the number of dissections, the number of quadrants with dissections; the length of edge dissections; and the number of dissections at the borders were significantly associated with the absolute number and delta value at 1 week number of CD133+/KDR+/CD45low (**Table 4**, **Figure 2B**).

Injury score was closely related to the maximal neointimal thickness at 9 months follow up (β 0.0008 [0.00004; 0.002]; P=0.04). and percentage maximal in-stent volume obstruction (β 0.0003 [0.00005; 0.006]; P=0.02) (**Figure 2D**). A trend was noted between the number of dissections at the borders and the maximal in-stent volume obstruction, and number of in-stent dissections and maximal neointi-

Table 2. Optical Coherence Tomography Parameters

	Post-procedure (N=24)	9-month follow up (N=21)	P value
Mean LA, mm^2	7.56±1.94	7.07±2.2	0.015
Minimal LA, mm^2	5.93±1.82	5.33±2.0	0.015
Mean stent area, mm^2	7.68±2.12	7.90±2.3	0.064
Minimal stent area, mm^2	6.23±2.04	6.35±2.2	0.39
Mean ISA area, mm^2	0.41±0.24	0.19±0.5	0.024
LA in proximal segment	8.55±2.74	8.90±4.2	0.74
LA in distal segment	6.19±2.89	6.03±2.7	0.62
Mean intima area , mm^2		0.84±0.5	
In-stent / stent area obstruction, %		10.91±5.4	
Maximal in-stent area obstruction, %		28.67±13.3	
Mean neointimal thickness, μm		101±49	
Maximal neointimal thickness, μm		426±189	
Mean neointimal volume, mm^3		18.17±13.76	
Percentage mean in-stent volume obstruction		243.52±161.48	
Percentage maximum in-stent volume obstruction		651.94±447.16	

Data are presented as mean±SD. ISA, incomplete stent apposition; LA, luminal area.

Table 3. Classification of Stent Strut Condition at 9 Months Follow up

	Everolimus-eluting stent (no. of struts)	Percentage
Well-apposed to the vessel wall with neointimal coverage	5,205	94.44
Well-apposed to the vessel wall without neointimal coverage	214	3.88
Malapposed to the vessel wall with neointimal coverage	6	0.10
Malapposed to the vessel wall without neointimal coverage	17	0.30
Orifice branch site with neointimal coverage	52	0.94
Orifice branch site without neointimal coverage	17	0.30

Table 4. Association Between CD133+/KDR+/CD45low Cells and Parameters of Vascular Damage After Stent Implantation Measured by OCT at 9 Months Follow up

OCT parameters of vessel injury	CD133+/KDR+/CD45low cells/μL at 1-week Number of CPC vs. OCT parameters	CD133+/KDR+/CD45low cells/μL Delta (1 week baseline) Number of CPC vs. OCT parameters
Thrombosis	0.29±0.63 vs. 0.033±0.08* β 0.0014 (–0.038; 0.04); P=0.946	0.144±0.72 vs. 0.033±0.08* β 0.006 (–0.032; 0.45); P=0.751
Number of prolapses	0.29±0.63 vs. 0.24±0.19* β 0.31 (0.16; 0.46); P<0.0001	0.144±0.72 vs. 0.24±0.19* β 0.05 (–0.10; 0.21); P=0.499
Number of cuandrants with prolapse	0.29±0.63 vs. 0.21±0.15* β –0.013 (0.07; 0.04); P=0.630	0.144±0.72 vs. 0.21±0.15* β 0.13 (0.084; 0.17); P<0.0001
Number of in-stent dissections	0.29±0.63 vs. 0.62±0.28* β 0.19 (0.09; 0.3); P<0.0001	0.144±0.72 vs. 0.62±0.28* β 0.17 (0.079; 0.27); P<0.0001
Number of cuandrants with in-stent dissections	0.29±0.63 vs. 0.60±0.27* β 0.19 (0.1; 0.29); P<0.0001	0.144±0.72 vs. 0.60±0.27* β 0.17 (0.091; 0.27); P<0.0001
Dissection length at the border	0.29±0.63 vs. 0.17±0.49* β 0.72 (0.53; 0.9); P<0.0001	0.144±0.72 vs. 0.17±0.49* β 0.64 (0.4; 0.9); P<0.0001
Number of FLAPs at the border	0.29±0.63 vs. 0.23±0.48* β 0.60 (0.36; 0.81); P<0.0001	0.144±0.72 vs. 0.23±0.48* β 0.53 (0.25; 0.81); P<0.0001
Vascular damage	0.29±0.63 vs. 1.28±0.76* β 0.84 (0.65; 1.03); P<0.0001	0.144±0.72 vs. 1.28±0.76* β 0.72 (0.43; 1.02); P<0.0001
Injury score	0.29±0.63 vs. 0.95±0.49* β 0.31 (0.16; 0.46); P<0.0001	0.144±0.72 vs. 0.95±0.49* β 0.28 (0.15; 0.41); P<0.0001

Data are presented as mean±SD. All comparisons were adjusted in a generalized estimating equations (GEE) model. OCT, optical coherence tomography.

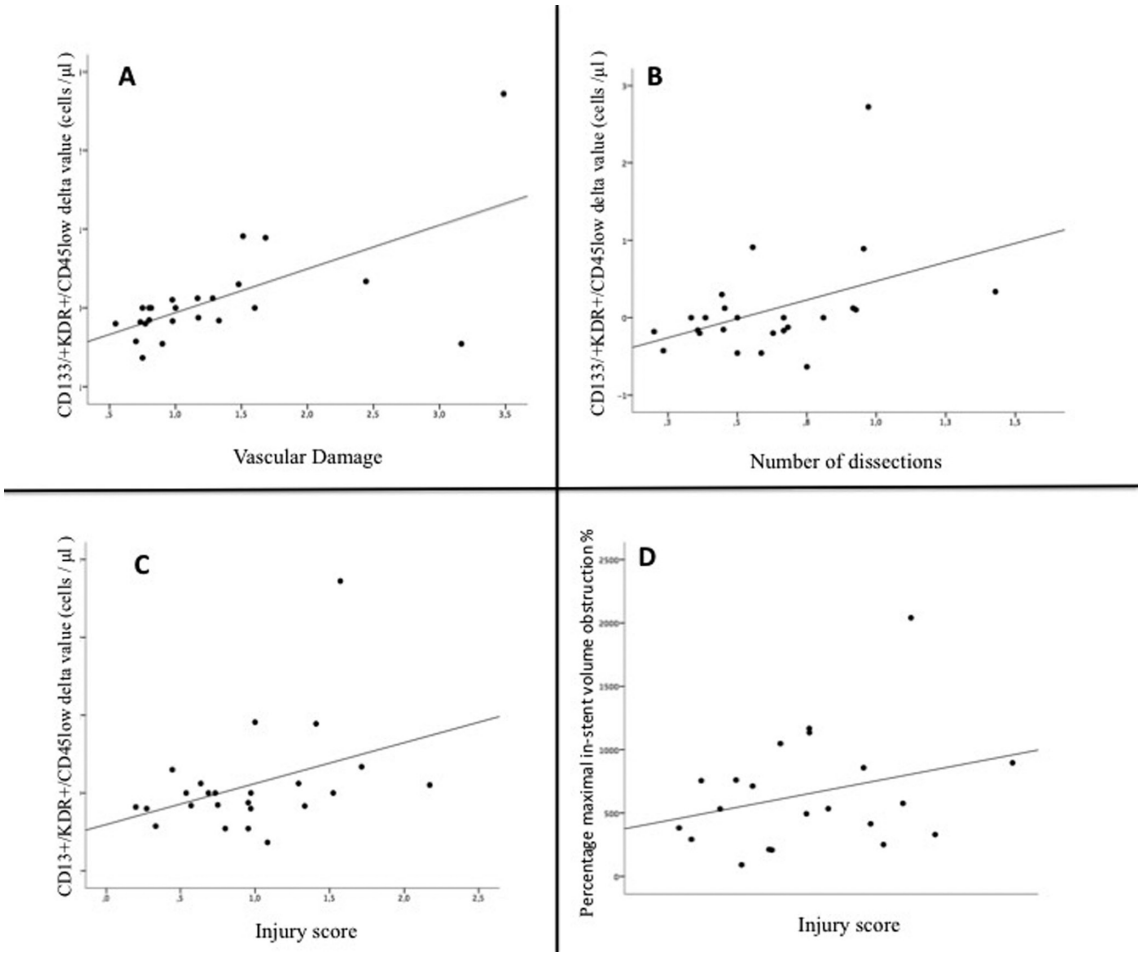

Figure 2. Scatterplot that shows the relationship between delta value at 1 week of CD133+/KDR+/CD45low and vascular damage (**A**), number of dissections (**B**) and injury sore (**C**). (**D**) Relationship between percentage maximal in-stent volume obstruction and injury score at 9 months.

mal thickness, but this did not reach statistical significance [β 0.0002 [−0.00006; 0.006]; P=0.10), (β 0.0003 [−0.0004; 0.0008]; P=0.08), respectively. In contrast, no significant association between injury score and mean neointimal area was observed (β −0.03 [−0.38–0.32]; P=0.856).

Moreover, an association between stent-to-vessel diameter ratio and injury and vascular damage score was statistically significant (β 1.07 [95% CI 0.31; 1.83]; P=0.006; β 1.2 [95% CI 0.29; 2.1]; P=0.01). In addition, a trend toward an association between CD133+/KDR+/CD45low and stent-to-vessel diameter ratio was also observed (β 0.05 [95% CI −0.02–0.13; 1.83]; P=0.1).

An inverse significant association between CPC functionality and OCT parameters of neointimal hyperplasia were observed. Baseline CFU were related to mean intima area (β −0.03 [−0.064; 0.004]; P=0.083), percentage of in-stent area obstruction (β −0.59 [−0.86; −0.32]; P<0.0001), percentage of maximal in-stent area obstruction (β −1.32 [−1.89; −0.075]; P<0.0001), and mean neointima thickness (mm; β −3.73 [−6.6; −0.82]; P=0.012).

An inverse relationship was also observed between the number of uncovered and apposed struts at 9 months and the delta value (1-week–baseline) of CD133+/KDR+/CD45low (β −12.53 [−22.17; −2.90]; P=0.011).

Discussion

The main findings of this pilot study provide new in vivo observations on the reparative vascular process taking place in coronary arteries treated with second-generation drug-eluting stents. Our research findings point toward a dynamic process; (1) we found a systemic response at 1 week proportional to the degree of vessel wall injury; (2) vessel wall injury degree measured by OCT and QCA yield a statistically significant association with in-stent neointimal growth at 9 months; (3) an impairment in CPC functionality was associated with the degree of neointimal hyperplasia; and (4) the lack of increase in CPC levels correlate with the degree of stent healing failure measured by strut coverage at 9 months.

The design of our study allowed for the identification of a relationship between vascular injury and CPC response, providing new clues on the activation of local and systemic mechanisms of vascular healing after EES implantation.

We found that both the injury score and the vascular damage score were associated with the increase at 1 week in the number of CD133+/KDR+/CD45low. One of the underlying mechanisms explaining a systemic response after acute vascular injury is the modification of local shear stress after stent implantation. Low local shear stress increases the permeability of the endothelium to circulating molecules, increases the expression of cell adhesion molecules and growth factors contributing to mobilisation of CPC, vessel inflammation, and smooth muscle cells proliferation. Both injury and vascular damage scores are based on multiple aspects of stent-related vessel damage (tissue prolapse, dissections located within the stented segment or at the edges of the stent, intraluminal thrombi) that have in common the disruption of laminar flow and the modification of shear stress at a stented segment.[18] Previous research has demonstrated that shear stress plays a key role in the endothelial PC differentiation,[19,20] and that signalling of that process occurs via the PI3k/Akt-SIRT1-Ac-H3 pathway.[20]

An interesting aspect in the study of neointimal formation following stent implantation is the qualitative assessment of neointimal tissue with OCT using normalised optical density. Previous studies have shown that it is possible to assess the maturity of the neointimal tissue with OCT and this correlated with histological findings.[21] In this regard, Nishino et al[22] found a significant correlation between mean neointimal area and mean neointimal thickness and neointimal maturity. Furthermore, when the neointimal maturity after BMS, ZES and EES was compared, the normalised optical density was lower in the EES group compared to the other types of stents. In this study, the maturity of neointimal tissue did not correlate with percentage changes in circulating endothelial progenitor cells (CD34+CD133+CD45 low cells) measured at follow up. We can speculate that one of the reasons for this may be the time point used to evaluate this biological response. The mobilisation of CPC levels occurs within the acute phase following stent deployment,[5] which is the time-point at which the repair mechanisms are most activated.

The clinical relevance of this study is based on the hypothesis that modification of vascular injury and repair processes is a key area in the development of novel therapies for atherosclerosis and the optimisation of endovascular interventions.[23] Recently published studies comparing 2 stents with different strut thicknesses have reinforced the importance of stent design in clinical outcomes.[24,25]

Two mechanisms for the positive results of these studies have been postulated; one of them is the stent design itself,[26] and the other is the degree of vascular injury-induced post stent implantation. Our study shows a correlation between the degree of vascular injury measured by OCT and QCA (balloon/artery ratio) and neointimal formation. This finding agrees with pivotal studies performed in the BMS era, reporting a proportional response between the degree of arterial injury and the severity of neointimal thickening in a porcine coronary model,[27] and in clinical studies using luminal gain as a surrogate of vascular injury during PCI.[28] The existence of such a relationship, together with the effects of systemic pathways of vessel healing, may explain the individual variability response secondary to EES implantation observed in the clinical setting.

Deep vessel wall injury stimulates local and systemic reparative mechanisms and bone marrow-derived cells might be an additional source of vascular cells that contribute to vascular repair, as suggested by numerous studies.[10,29] However, neointima formation is a consequence of excessive or a pathological healing process in response to vascular injury that may result in severe stenosis or even vessel occlusion (occlusive restenosis) with important clinical consequences.[30] Previous studies have shown that bone marrow-derived cells contributed to neointimal hyperplasia after endovascular injury; however, as yet, the multitude of mechanisms involved in the development of normal vascular repair, or a pathological vascular repair and their interactions, are not fully elucidated. This study shows, for the first time, the relationship between vessel injury following EES implantation and CPC response. We sincerely believe that this is relevant as it may shed light on the reparative process. CPC are known to mainly exert a paracrine effect and contribute to vascular repair, especially through the release of paracrine factors such as vascular endothelial growth factor (VEGF) or hepatocyte growth factor (HGF),[31] which may activate both resident endothelial cells and fibroblasts causing the development of neointimal hyperplasia. However, not only does the number of circulating cells influence neointimal formation, but there are also other known systemic factors associated with an increase in the risk of restenosis such as ageing,[32,33] diabetes mellitus, and renal impairment that may also affect the functionality of CPCs and therefore, may influence neointima formation. In fact, in the present study, we evaluated the number of CFUs, which is a way to evaluate the functionality of the CPC, and this showed a significant, but inverse, association with the amount of neointimal hyperplasia.

In the long term, the percentage of covered struts is lower in EES, compared with BMS,[34] which may be explained by 2 mechanisms: the local inhibiting effect of everolimus on endothelial cell proliferation and differentiation; and a systemic effect secondary to the drug release from the stented segment to the bloodstream,[35] with a potential direct effect on bone marrow.[36] The latter mechanism also explains our finding of an inverse relationship between the number of uncoated and apposed struts at 9 months and the increase at 1 week in CPCs levels of endothelial lineage (CD133+/KDR+/CD45low). Other factors that affect the regenerative capacity of the bone marrow may also affect the BM-PC response to a vascular injury.[32,33,37]

Study Limitations

The major limitation of this pilot study is its sample size and in the fact that only 20 patients (24 lesions) entered the study over a 2-year period. This is due to the fact that we have limited time to use flow cytometry analysis for research. The present study included a small sample and therefore the results must be considered hypothesis-generating and interpreted with caution. Based on the results of the first 9 patients included in the study, we calculated a sample size of 19 patients. For this reason and given that the protocol required a second routine catheterisation for study purposes only, we did not include additional patients. The characterisation of CPCs is still under debate and there is no consensus on the best definition of endothelial progenitor cell subsets due to variations in isolation strategies and inconsistencies in the use of lineage markers. The present study applied the widely used method based on analysis of a surface marker for progenitor cells. The relationship between CPC levels and neointimal growth shown in the study is only based on the circulating CPC; we did not measure CPC levels locally at the level of the coronary

stent, so therefore origin of the intimal cells and the contribution of CPC to neointimal hyperplasia are unknown. Eventually, labelling CPC in experimental animal models could be helpful in this regard. Severely calcified lesions that required the use of ablation techniques (i.e., rotational atherectomy) were excluded from the study. Thus, the association observed between vessel injury and CPCs cannot be extrapolated to this specific type of lesions. All patients included were on chronic treatment with statins and ACEi/ARBs. Although the protocol recommended avoiding the introduction of additional drugs that can influence the mobilisation of CPCs, such as anti-anginal treatment at least in the first month following PCI, this was left to the attending physician's discretion.

Conclusions

In conclusion, this study found a systemic response proportional to the degree of vessel wall injury and a link between vessel injury and the development of neointimal hyperplasia following EES implantation. In addition, impairment in CPC functionality was associated with the degree of neointimal hyperplasia. Finally, a lack of an early increase in CPCs, and the degree of strut coverage at 9 months following EES implantation, has been documented. However, this is a study with a small sample size and therefore more studies are required to confirm these promising results. Thus, decreasing the rate of DES failure will require focused efforts to decrease vascular damage caused during stent implantation by improving stent designs (i.e., struts thickness, polymer coating) and optimising stent deployment. In addition, enhanced vascular systemic regenerative capacity includes improving CPC and endothelial function by controlling cardiovascular risk factors.

Disclosures

The authors declare no conflicts of interest.

Sources of Funding

P.J.-Q. received the Instituto de Salud Carlos III (ISCIII) "Fondo de Investigación Sanitaria" grant (PI11/00299) to perform this study. The study was also partially financed by the BIOMEDICAL RESEARCH scholarship of the Eugenio Rodriguez Pascual Foundation and Fundación Interhospitalaria para la Investigación Cardiovascular.

Samples were obtained from San Carlos Clinical Hospital Biobank (B.000072) belonging to the San Carlos Health Care Research Institute (IdISSC), which is part of the national network of Biobanks project subsidized by ISCIII (PT17 / 0015/0040) and co-financed by the European fund for regional development / European social fund (ERDF).

IRB Information

The Ethics Committee of the Hospital Clinico San Carlos (Reference number: 11-126-E) approved this study. Clinical Trial Registration: NCT03214900.

References

1. Spione F, Brugaletta S. Second generation drug-eluting stents: A focus on safety and efficacy of current devices. *Expert Rev Cardiovasc Ther* 2021; **19:** 107–127.
2. Schwartz RS, Huber KC, Murphy JG, Edwards WD, Camrud AR, Vlietstra RE, et al. Restenosis and the proportional neointimal response to coronary artery injury: Results in a porcine model. *J Am Coll Cardiol* 1992; **19:** 267–274.
3. Asahara T, Murohara T, Sullivan A, Silver M, van der Zee R, Li T, et al. Isolation of putative progenitor endothelial cells for angiogenesis. *Science* 1997; **275:** 964–967.
4. Tsai S, Butler J, Rafii S, Liu B, Kent KC. The role of progenitor cells in the development of intimal hyperplasia. *J Vasc Surg* 2009; **49:** 502–510.
5. Inoue T, Sata M, Hikichi Y, Sohma R, Fukuda D, Uchida T, et al. Mobilization of CD34-positive bone marrow-derived cells after coronary stent implantation: Impact on restenosis. *Circulation* 2007; **115:** 553–561.
6. Pelliccia F, Cianfrocca C, Rosano G, Mercuro G, Speciale G, Pasceri V. Role of endothelial progenitor cells in restenosis and progression of coronary atherosclerosis after percutaneous coronary intervention: A prospective study. *JACC Cardiovasc Interv* 2010; **3:** 78–86.
7. George J, Herz I, Goldstein E, Abashidze S, Deutch V, Finkelstein A, et al. Number and adhesive properties of circulating endothelial progenitor cells in patients with in-stent restenosis. *Arterioscler Thromb Vasc Biol* 2003; **23:** e57–e60.
8. Lei LC, Huo Y, Li JP, Li XX, Han YY, Wang HZ, et al. Activities of circulating endothelial progenitor cells in patients with in-stent restenosis. *Zhonghua Yi Xue Za Zhi* 2007; **87:** 3394–3398 (in Chinese).
9. Simper D, Stalboerger PG, Panetta CJ, Wang S, Caplice NM. Smooth muscle progenitor cells in human blood. *Circulation* 2002; **106:** 1199–1204.
10. Tanaka K, Sata M, Hirata Y, Nagai R. Diverse contribution of bone marrow cells to neointimal hyperplasia after mechanical vascular injuries. *Circ Res* 2003; **93:** 783–790.
11. Schmidt-Lucke C, Fichtlscherer S, Aicher A, Tschöpe C, Schultheiss HP, Zeiher AM, et al. Quantification of circulating endothelial progenitor cells using the modified ISHAGE protocol. *PLoS One* 2010; **5:** e13790.
12. Rixe J, Rolf A, Conradi G, Moellmann H, Nef H, Neumann T, et al. Detection of relevant coronary artery disease using dual-source computed tomography in a high probability patient series: Comparison with invasive angiography. *Circ J* 2009; **73:** 316–322.
13. Gutiérrez-Chico JL, Wykrzykowska J, Nüesch E, van Geuns RJ, Koch KT, Koolen JJ, et al. Vascular tissue reaction to acute malapposition in human coronary arteries: Sequential assessment with optical coherence tomography. *Circ Cardiovasc Interv* 2012; **5:** 20–29; S1–S8.
14. Inoue T, Shite J, Yoon J, Shinke T, Otake H, Sawada T, et al. Optical coherence evaluation of everolimus-eluting stents 8 months after implantation. *Heart* 2011; **97:** 1379–1384.
15. Gonzalo N, Serruys PW, Okamura T, Shen ZJ, Onuma Y, Garcia-Garcia HM, et al. Optical coherence tomography assessment of the acute effects of stent implantation on the vessel wall: A systematic quantitative approach. *Heart* 2009; **95:** 1913–1919.
16. Vilchez-Tschischke JP, Salazar C, Gil-Romero J, Mori R, Nuñez-Gil I, Quirós A, et al. Stent strut thickness and acute vessel injury during percutaneous coronary interventions: An optical coherence tomography randomized clinical trial. *Coron Artery Dis* 2021; **32:** 382–390.
17. Alfonso F, Sandoval J, Pérez-Vizcayno MJ, Cárdenas A, Gonzalo N, Jiménez-Quevedo P, et al. Mechanisms of balloon angioplasty and repeat stenting in patients with drug-eluting in-stent restenosis. *Int J Cardiol* 2015; **178:** 213–220.
18. Ng J, Bourantas CV, Torii R, Ang HY, Tenekecioglu E, Serruys PW, et al. Local hemodynamic forces after stenting: Implications on restenosis and thrombosis. *Arterioscler Thromb Vasc Biol* 2017; **37:** 2231–2242.
19. Wang H, Riha GM, Yan S, Li M, Chai H, Yang H, et al. Shear stress induces endothelial differentiation from a murine embryonic mesenchymal progenitor cell line. *Arterioscler Thromb Vasc Biol* 2005; **25:** 1817–1823.
20. Cheng BB, Yan ZQ, Yao QP, Shen BR, Wang JY, Gao LZ, et al. Association of SIRT1 expression with shear stress induced endothelial progenitor differentiation. *J Cell Biochem* 2012; **113:** 3663–3671.
21. Templin C, Meyer M, Müller MF, Djonov V, Hlushchuk R, Dimova I, et al. Coronary optical frequency domain imaging (OFDI) for in vivo evaluation of stent healing: Comparison with light and electron microscopy. *Eur Heart J* 2010; **31:** 1792–1801.
22. Nishino S, Sakuma M, Kanaya T, Nasuno T, Tokura M, Toyoda S, et al. Neointimal tissue characterization after implantation of drug-eluting stents by optical coherence tomography: Quantitative analysis of optical density. *Int J Cardiovasc Imaging* 2019; **35:** 1971–1978.
23. Foin N, Lee RD, Torii R, Guitierrez-Chico JL, Mattesini A, Nijjer S, et al. Impact of stent strut design in metallic stents and biodegradable scaffolds. *Int J Cardiol* 2014; **177:** 800–808.
24. Menown IBA, Mamas MA, Cotton JM, Hildick-Smith D, Eberli FR, Leibundgut G, et al. Thin strut CoCr biodegradable poly-

mer biolimus A9-eluting stents versus thicker strut stainless steel biodegradable polymer biolimus A9-eluting stents: Two-year clinical outcomes. *J Interv Cardiol* 2021; **2021:** 6654515.
25. Madhavan MV, Howard JP, Naqvi A, Ben-Yehuda O, Redfors B, Prasad M, et al. Long-term follow-up after ultrathin vs. conventional 2nd-generation drug-eluting stents: A systematic review and meta-analysis of randomized controlled trials. *Eur Heart J* 2021; **42:** 2643–2654.
26. Garasic JM, Edelman ER, Squire JC, Seifert P, Williams MS, Rogers C. Stent and artery geometry determine intimal thickening independent of arterial injury. *Circulation* 2000; **101:** 812–818.
27. Cole CW, Hagen PO, Lucas JF, Mikat EM, O'Malley MK, Radic ZS, et al. Association of polymorphonuclear leukocytes with sites of aortic catheter-induced injury in rabbits. *Atherosclerosis* 1987; **67:** 229–236.
28. Beatt KJ, Serruys PW, Luijten HE, Rensing BJ, Suryapranata H, de Feyter P, et al. Restenosis after coronary angioplasty: The paradox of increased lumen diameter and restenosis. *J Am Coll Cardiol* 1992; **19:** 258–266.
29. Shoji M, Sata M, Fukuda D, Tanaka K, Sato T, Iso Y, et al. Temporal and spatial characterization of cellular constituents during neointimal hyperplasia after vascular injury: Potential contribution of bone-marrow-derived progenitors to arterial remodeling. *Cardiovasc Pathol* 2004; **13:** 306–312.
30. Mishkel GJ, Moore AL, Markwell S, Shelton MC, Shelton ME. Long-term outcomes after management of restenosis or thrombosis of drug-eluting stents. *J Am Coll Cardiol* 2007; **49:** 181–184.
31. Rehman J, Li J, Orschell CM, March KL. Peripheral blood "endothelial progenitor cells" are derived from monocyte / macrophages and secrete angiogenic growth factors. *Circulation* 2003; **107:** 1164–1169.
32. Hammadah M, Al Mheid I, Wilmot K, Ramadan R, Abdelhadi N, Alkhoder A, et al. Telomere shortening, regenerative capacity, and cardiovascular outcomes. *Circ Res* 2017; **120:** 1130–1138.
33. Hill JM, Zalos G, Halcox JP, Schenke WH, Waclawiw MA, Quyyumi AA, et al. Circulating endothelial progenitor cells, vascular function, and cardiovascular risk. *N Engl J Med* 2003; **348:** 593–600.
34. Sakuma M, Nasuno T, Abe S, Obi S, Toyoda S, Taguchi I, et al. Mobilization of progenitor cells and assessment of vessel healing after second generation drug-eluting stenting by optical coherence tomography. *Int J Cardiol Heart Vasc* 2018; **18:** 17–24.
35. Wiemer M, Seth A, Chandra P, Neuzner J, Richardt G, Piek JJ, et al. Systemic exposure of everolimus after stent implantation: A pharmacokinetic study. *Am Heart J* 2008; **156:** 751.e1–e7.
36. Tie G, Messina KE, Yan J, Messina JA, Messina LM. Hypercholesterolemia induces oxidant stress that accelerates the ageing of hematopoietic stem cells. *J Am Heart Assoc* 2014; **3:** e000241.
37. Marx SO, Totary-Jain H, Marks AR. Vascular smooth muscle cell proliferation in restenosis. *Circ Cardiovasc Interv* 2011; **4:** 104–111.